CHAPTER 4.

Drought and Moisture Surplus Patterns in the Conterminous United States: 2018, 2016–2018, and 2014–2018

Frank H. Koch
John W. Coulston

INTRODUCTION

Although ecologists do not define the term "drought" consistently (Slette and others 2019), one definition that is applicable to forests is that a drought is a period of precipitation deficit that persists long enough to deplete available soil water, leading to impacts on trees and other plants; in some cases, these impacts include plant injury or death (Anderegg and others 2012, Hanson and Weltzin 2000). Under this definition, droughts affect most forests in the United States, but their frequency and intensity vary considerably between geographic regions (Hanson and Weltzin 2000). These variations define the regions' predominant drought regimes. Most forests in the Western United States are subject to seasonal droughts on a yearly basis. By comparison, forests in the Eastern United States usually exhibit one of the following drought patterns: random (i.e., occurring at any time of year) occasional droughts, as usually observed in the Appalachian Mountains and the Northeast, or frequent late-summer droughts, as usually observed in the Southeastern Coastal Plain and the eastern portion of the Great Plains (Hanson and Weltzin 2000).

In forests, moisture scarcity during droughts can cause considerable tree stress, especially when that scarcity co-occurs with periods of high temperatures (L.D.L. Anderegg and others 2013, Peters and others 2015, Williams and others 2013). Trees and other plants react to this stress by decreasing fundamental growth processes such as cell division and enlargement. Because photosynthesis is less sensitive than these fundamental processes, it decreases slowly at low levels of drought stress but decreases more rapidly as the stress becomes more severe (Kareiva and others 1993, Mattson and Haack 1987). Ultimately, prolonged drought stress can lead to failure of a tree's hydraulic system, resulting in crown death and subsequent tree mortality (Choat and others 2018). In addition to these direct effects, drought stress often makes trees vulnerable to attack by damaging insects and diseases (Clinton and others 1993, Kolb and others 2016, Mattson and Haack 1987, Raffa and others 2008). Droughts also increase wildland fire risk by inhibiting breakdown of organic matter and diminishing the moisture content of downed woody debris and other potential fire fuels (Clark 1989, Keetch and Byram 1968, Schoennagel and others 2004, Trouet and others 2010).

Most forest systems are resistant to short-term droughts, although individual tree species differ in their degree of drought tolerance (Archaux and Wolters 2006, Berdanier and Clark 2016). Because of this resistance, drought duration may be a more critical factor for forests than drought intensity (Archaux and Wolters 2006). For example, forests that experience multiple consecutive years of drought (2–5 years) are much more likely to have high tree mortality than forests that experience a single year of extreme drought (Guarín and Taylor 2005, Millar and others 2007). Indeed, the latter period is probably short enough that any impacts of the drought on tree growth and function are still reversible (Bigler and others 2006). Stated differently, forests may have to be subjected to a prolonged period of comparatively intense drought conditions before they experience effects similar to those observed with shorter term droughts in other (e.g., rangeland) systems. Therefore, a thorough evaluation of drought impact in forests should include analysis of moisture conditions over multiyear time windows.

In the 2010 Forest Health Monitoring (FHM) annual national report, we described a method for mapping drought conditions across the conterminous United States (Koch and others 2013b). Our objective was to generate fine-scale, drought-related spatial datasets that improve upon similar products available from sources such as the National Oceanic and Atmospheric Administration's National Centers for Environmental Information (e.g., Vose and others 2014) or the U.S. Drought Monitor program (Svoboda and others 2002). The primary inputs are gridded climate data (i.e., monthly raster maps of precipitation and temperature over a 100-year period) created with the Parameter-elevation Regression on Independent Slopes (PRISM) climate mapping system (Daly and others 2002). The method uses a standardized indexing approach that facilitates comparison of a given location's moisture status during different time windows, regardless of their length. The index is more straightforward to calculate than the commonly used Palmer Drought Severity Index, or PDSI (Palmer 1965), and avoids some criticisms of the PDSI (see Alley 1984) regarding its underlying assumptions and limited comparability across space and time. Here, we applied the method outlined in the 2010 FHM report to the most currently available climate data (i.e., the monthly PRISM data through 2018), thereby providing the tenth installment in an ongoing series of annual drought assessments for the conterminous United States from 2009 forward (Koch and Coulston 2015, 2016, 2017, 2018, 2019; Koch and others 2013a, 2013b, 2014, 2015).

This is the fifth year in which we also mapped levels of moisture surplus across the conterminous United States during multiple time windows. While recent refereed literature (e.g., Adams and others 2009, Allen and others 2010, Martínez-Vilalta and others 2012, Peng and others 2011, Williams and others 2013) has usually focused on reports of regional-scale forest decline and mortality due to persistent drought conditions, especially in combination with periods of extremely high temperatures (i.e., heat waves), surplus moisture availability can also be damaging to forests. Abnormally high moisture can be a short-term stressor (e.g., an extreme rainfall event with subsequent flooding) or a long-term stressor (e.g., persistent wetness caused by a macroscale climatic pattern such as the El Niño-Southern Oscillation), either of which may lead to tree dieback and mortality (Rozas and García-González 2012, Rozas and Sampedro 2013). Such impacts have been observed in both tropical and temperate forests (Hubbart and others 2016, Laurance and others 2009, Rozas and García-González 2012). While surplus-induced impacts in forests may not be as common as drought-induced impacts, a single index that depicts both moisture surplus and deficit conditions provides a more complete indicator of potential forest health issues.

METHODS

We acquired grids for monthly precipitation and monthly mean temperature for the conterminous United States from the PRISM Climate Group website (PRISM Climate Group 2019). At the time of these analyses, gridded datasets were available for all years from 1895 to 2018. The spatial resolution of the grids was approximately 4 km (cell area = 16 km^2). For future applications and to ensure better compatibility with other spatial datasets, all output grids were resampled to a spatial resolution of approximately 2 km (cell area = 4 km^2) using a nearest neighbor approach. The nearest neighbor approach is a computationally simple resampling method that avoids the smoothing of data values observed with methods such as bilinear interpolation or cubic convolution.

Potential Evapotranspiration (PET) Maps

As in our previous drought mapping efforts (Koch and Coulston 2015, 2016, 2017, 2018, 2019; Koch and others 2012a, 2012b, 2013a, 2013b, 2014, 2015), we adopted an approach in which a moisture index value is calculated for each location of interest (i.e., each grid cell in a map of the conterminous United States) during a given time period. Moisture indices are intended to reflect the amount of available water in a location (e.g., to support plant growth). In our case, the index is computed using an approach that considers both the amount of precipitation that falls on a location during the period of interest as well as the level of potential evapotranspiration during this period. Potential evapotranspiration measures the loss of soil moisture through plant uptake and transpiration (Akin 1991). It does not measure actual moisture loss, but rather the loss that would occur if there was no possible shortage of moisture for plants to transpire (Akin 1991, Thornthwaite 1948). Potential evapotranspiration serves as a basic measure of moisture demand. By incorporating potential evapotranspiration along with precipitation, our index thus documents the long-term balance between moisture demand and supply for each location of interest.

To complement the available PRISM monthly precipitation grids, we computed monthly potential evapotranspiration (*PET*) grids using Thornthwaite's formula (Akin 1991, Thornthwaite 1948):

$$PET_m = 1.6L_{lm}(10\frac{T_m}{I})^a \qquad (1)$$

where

PET_m = the potential evapotranspiration for a given month *m* in cm

L_{lm} = a correction factor for the mean possible duration of sunlight during month *m* for all locations (i.e., grid cells) at a particular latitude *l* (see Table V in Thornthwaite [1948] for a list of *L* correction factors by month and latitude)

T_m = the mean temperature for month *m* in degrees C

I = an annual heat index, calculated as

$$I = \sum_{m=1}^{12}\left(\frac{T_m}{5}\right)^{1.514}$$

where

T_m is the mean temperature for each month *m* of the year

a = an exponent calculated as $a = 6.75 \times 10^{-7} I^3 - 7.71 \times 10^{-5} I^2 + 1.792 \times 10^{-2} I + 0.49239$ (see Appendix I in Thornthwaite [1948] regarding calculation of *I* and the empirical derivation of *a*)

Although only a simple approximation, a key advantage of Thornthwaite's formula is that it has modest input data requirements (i.e., mean temperature values) compared to more sophisticated methods of estimating *PET* such as the Penman-Monteith equation (Monteith 1965), which requires less readily available data on factors such as humidity, radiation, and wind speed. To implement equation (1) spatially, we created a grid of latitude values for determining the *L* adjustment for any given grid cell (and any given month) in the conterminous United States. We extracted the T_m values for the grid cells from the corresponding PRISM mean monthly temperature grids.

Moisture Index Maps

To estimate baseline conditions, we used the precipitation (*P*) and *PET* grids to generate moisture index grids for the past 100 years (i.e., 1919–2018) for the conterminous United States. We used a moisture index described by Willmott and Feddema (1992), which has been applied in a variety of contexts, including global vegetation modeling (Potter and Klooster 1999) and climate change analysis (Grundstein 2009). Willmott and Feddema (1992) devised the index as a refinement of one described earlier by Thornthwaite (1948) and Thornthwaite and Mather (1955). Their revised index, *MI′*, has the following form:

$$MI' = \begin{cases} P/PET - 1 & , \quad P < PET \\ 1 - PET/P & , \quad P \geq PET \\ 0 & , \quad P = PET = 0 \end{cases} \qquad (2)$$

where

P = precipitation

PET = potential evapotranspiration, as calculated using equation (1)

(P and PET must be in equivalent measurement units, e.g., mm)

This set of equations yields a symmetric, dimensionless index scaled between -1 and 1. A primary advantage of this symmetry is that it enables valid comparisons between any set of locations in terms of their moisture balance (i.e., the balance between moisture demand and supply). MI' can be calculated for any time period but is commonly calculated on an annual basis using P and PET values summed across the entire year (Willmott and Feddema 1992). An alternative to this summation approach is to calculate MI' on a monthly basis (i.e., from total measured precipitation and estimated potential evapotranspiration in each month), and then, for a given time window of interest, calculate its moisture index as the mean of the MI' values for all months in the time window. This "mean-of-months" approach limits the ability of short-term peaks in either precipitation or potential evapotranspiration to negate corresponding short-term deficits, as would happen under a summation approach.

For each year in our study period (i.e., 1919–2018), we used the mean-of-months approach to calculate moisture index grids for three different time windows: 1 year (MI_1'), 3 years (MI_3'), and 5 years (MI_5'). Briefly, the MI_1' grids are the mean (i.e., the mean value for each grid cell) of the 12 monthly MI' grids for each year in the study period, the MI_3' grids are the mean of the 36 monthly grids from January 2 years prior through December of the target year, and the MI_5' grids are the mean of the 60 consecutive monthly MI' grids from January 4 years prior to December of the target year. Thus, the MI_1' grid for the year 2018 is the mean of the monthly MI' grids from January to December 2018, while the MI_3' grid is the mean of the grids from January 2016 to December 2018, and the MI_5' grid is the mean of the grids from January 2014 to December 2018.

Annual and Multiyear Drought Maps

To determine degree of departure from typical moisture conditions, we first created a normal grid, $MI'_{i\,norm}$, for each of our three time windows, representing the mean (i.e., the mean value for each grid cell) of the 100 corresponding moisture index grids (i.e., the MI_1', MI_3', or MI_5' grids, depending on the window; see fig. 4.1). We also created a standard deviation grid, $MI'_{i\,SD}$, for each time window, calculated from the window's 100 individual moisture index grids as well as its $MI'_{i\,norm}$ grid. We subsequently calculated moisture difference z-scores, MDZ_{ij}, for each time window using these derived datasets:

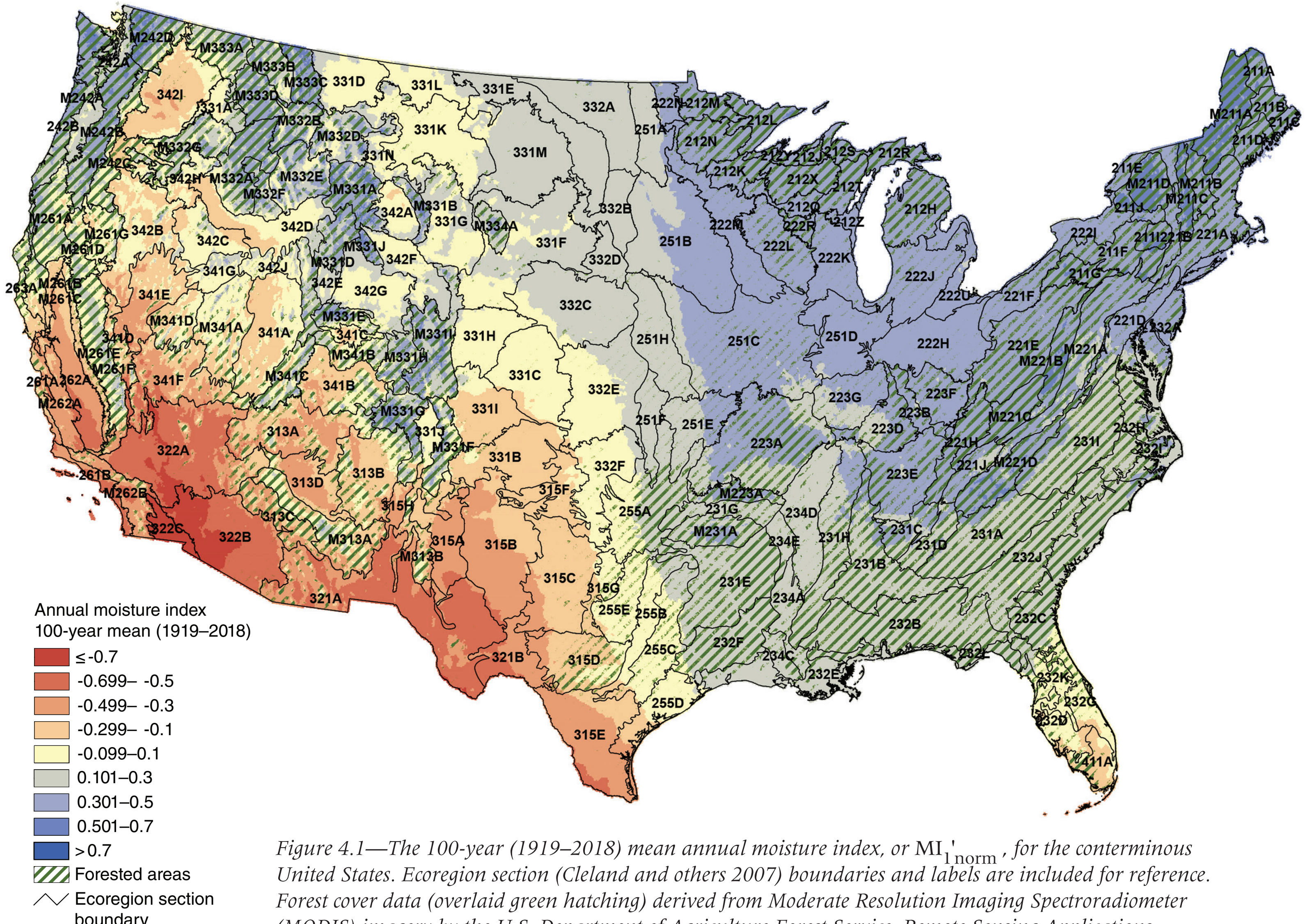

Figure 4.1—The 100-year (1919–2018) mean annual moisture index, or $MI_{1}{'}_{norm}$, for the conterminous United States. Ecoregion section (Cleland and others 2007) boundaries and labels are included for reference. Forest cover data (overlaid green hatching) derived from Moderate Resolution Imaging Spectroradiometer (MODIS) imagery by the U.S. Department of Agriculture Forest Service, Remote Sensing Applications Center. (Data source: PRISM Group, Oregon State University)

$$MDZ_{ij} = \frac{MI_i' - MI_{i\ norm}'}{MI_{i\ SD}'} \qquad (3)$$

where

i = the analytical time window (i.e., 1, 3, or 5 years) and *j* = a particular target year in our 100-year study period (i.e., 1919–2018)

MDZ scores may be classified in terms of degree of moisture deficit or surplus (table 4.1). The classification scheme includes categories (e.g., severe drought, extreme drought) like those associated with the PDSI. The scheme has also been adopted for other drought indices such as the Standardized Precipitation Index, or SPI (McKee and others 1993). Moreover, the breakpoints between *MDZ* categories resemble those used for the SPI, such that we expect the *MDZ* categories to have theoretical frequencies of occurrence that are similar to their SPI counterparts (e.g., approximately 2.3 percent of the time for extreme drought; see McKee and others 1993, Steinemann 2003). More importantly, because of the standardization in equation (3), the breakpoints between categories remain the same regardless of the size of the time window of interest. For comparative analysis, we generated and classified *MDZ* maps of the conterminous United States, based on all three time windows, for the target year 2018.

Table 4.1—Moisture difference *z*-score (*MDZ*) value ranges for nine wetness and drought categories, along with each category's approximate theoretical frequency of occurrence

MDZ	Category	Frequency
≤-2	Extreme drought	2.3%
-1.999 to -1.5	Severe drought	4.4%
-1.499 to -1	Moderate drought	9.2%
-0.999 to -0.5	Mild drought	15.0%
-0.499 to 0.5	Near normal conditions	38.2%
0.501 to 1	Mild moisture surplus	15.0%
1.001 to 1.5	Moderate moisture surplus	9.2%
1.501 to 2	Severe moisture surplus	4.4%
>2	Extreme moisture surplus	2.3%

RESULTS AND DISCUSSION

The 100-year (1919–2018) mean annual moisture index, or $MI_1'{}_{norm}$, grid (fig. 4.1) serves as a synopsis of moisture regimes in the conterminous United States. (The 100-year $MI_3'{}_{norm}$ and $MI_5'{}_{norm}$ grids were very similar to the mean $MI_1'{}_{norm}$ grid, and so are not shown here.) Wet climates (*MI'* >0) are typical in the Eastern United States, especially the Northeast. An anomaly worth noting is southern Florida, primarily ecoregion sections (Cleland and others 2007) 232D–Florida Coastal Lowlands-Gulf, 232G–Florida Coastal Lowlands-Atlantic, and 411A–Everglades. This region appears to be dry relative to other parts of the East, which is an effect of its tropical climate, which has distinct wet (primarily summer months) and dry (late fall to early spring) seasons. Although southern Florida usually receives a high level of precipitation during the wet season, it can be insufficient to offset the region's lengthy dry season (Duever and others 1994) or its high level of temperature-driven evapotranspiration, especially during the late spring and summer months, resulting in negative *MI′* values. This differs markedly from the pattern observed in the driest parts of the Western United States, especially the Southwest (e.g., sections 322A–Mojave Desert, 322B–Sonoran Desert, and 322C–Colorado Desert), where potential evapotranspiration is very high, as in southern Florida, but precipitation levels are typically very low. In fact, because of generally lower precipitation than the East, dry climates (*MI′* <0) are typical across much of the Western United States. Nevertheless, mountainous areas in the central and northern Rocky Mountains as well as the Pacific Northwest are relatively wet, such as ecoregion sections M242A–Oregon and Washington Coast Ranges, M242B–Western Cascades, M331G–South Central Highlands, and M333C–Northern Rockies. This is driven in part by large amounts of winter snowfall in these regions (Hanson and Weltzin 2000).

Figure 4.2 shows the annual (i.e., 1-year) *MDZ* map for 2018 for the conterminous United States. The map shows substantial contrast between the eastern and western portions of the country. From the Rocky Mountains westward, a majority of forested areas experienced at least mild drought (*MDZ* ≤-0.5) conditions in 2018, meaning that conditions were noticeably drier than normal in regions that already have dry moisture regimes (see fig. 4.1). Yet, contiguous areas of severe to extreme drought (*MDZ* ≤-1.5) were limited in number and geographic extent. Ecoregion sections in the West with the most noticeable concentrations of severe to extreme drought during 2018 included M242B–Western Cascades, portions of M242A–Oregon and Washington Coast Ranges and M261A–Klamath Mountains, and the northwestern corner of M333C–Northern Rockies, immediately adjacent to the United States-Canada border. There were other areas of severe to extreme drought in the central Rockies: ecoregion sections M331G–South Central Highlands, M331H–North Central Highlands and Rocky Mountains, and M331I–Northern Parks and Ranges. Similarly sized clusters of severe to extreme drought appeared in nearby sections 313B–Navajo Canyonlands and 313D–Painted Desert, but they occurred in areas with little forest cover.

In the Eastern United States, drought conditions during 2018 were largely confined to two geographic areas: northern New England and southern Florida. In the former region, small pockets of moderate drought (-1.5 < *MDZ* ≤ -1) were interspersed with a mix of mild surplus to mild drought conditions (-1 < *MDZ* ≤ 1). Ecoregion sections exhibiting this pattern included M211A–White Mountains, M211B–New England Piedmont, M211C–Green-Taconic-Berkshire Mountains, and M211D–Adirondack Highlands. In southern Florida, a significant cluster of severe to extreme drought appeared in section 411A–Everglades, while moderate to severe drought conditions occurred in 232G–Florida Coastal Lowlands-Atlantic, particularly along portions of the Atlantic

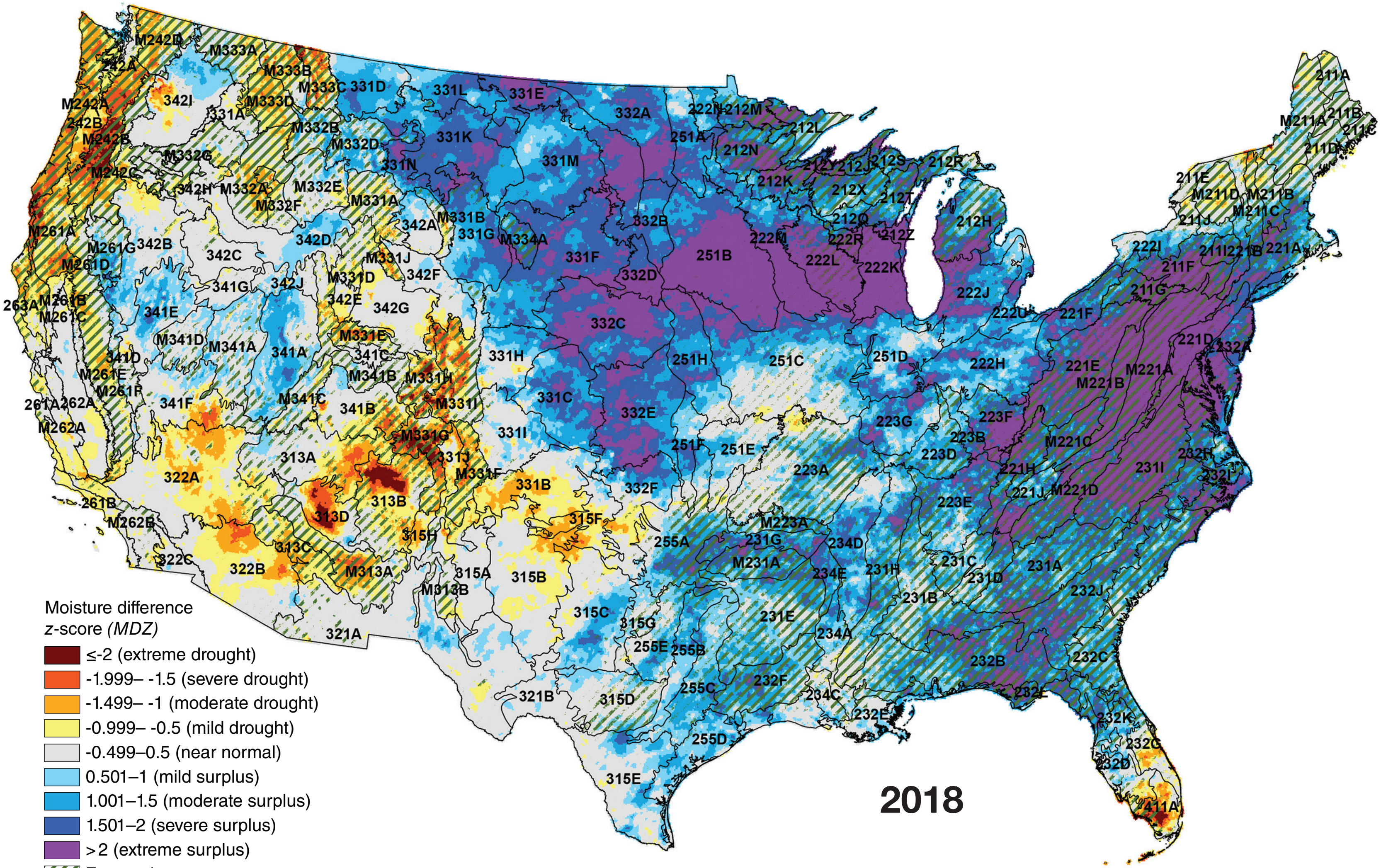

Figure 4.2—The 2018 annual (i.e., 1-year) moisture difference z-score, or MDZ, *for the conterminous United States. Ecoregion section (Cleland and others 2007) boundaries and labels are included for reference. Forest cover data (overlaid green hatching) derived from MODIS imagery by the U.S. Department of Agriculture Forest Service, Remote Sensing Applications Center. (Data source: PRISM Group, Oregon State University)*

coastline. Superficially, these two drought hot spots may appear to be similar, but it is worth recalling that, as depicted by the $MI_1'_{norm}$ grid (fig. 4.1), southern Florida has a drier moisture regime than virtually all other regions of the Eastern United States, including northern New England. Elsewhere in the East, moisture surplus conditions were widespread during 2018, including large contiguous areas of extreme surplus (*MDZ* >2) in the Mid-Atlantic and northern Great Plains regions.

Overall, the 2018 *MDZ* map (fig. 4.2) is consistent with summary metrics reported for the year (NOAA NCEI 2019). For example, the percentage of the country that was very dry was close to zero from October through December, while at the same time the percentage that was very wet ranged from approximately 13 percent to approximately 30 percent. Drought conditions were most extreme during spring (April–June) and most extensive geographically from July through September, but these were offset by unusually wet conditions in the latter portion of the year.

At a regional scale, moisture conditions in the Southwestern United States appeared to improve substantially in 2018 compared to 2017 (fig. 4.3), when a large contiguous zone of extreme drought (*MDZ* ≤-2) encompassed almost all of the "Four Corners" region (southeastern Utah, southwestern Colorado, northwestern New Mexico, and northeastern Arizona). This apparent improvement belies the fact that 2018 was the warmest year on record for the Southwest and represents the continuation of a 40-year warming trend that is likely to allow moderate or worse drought conditions to persist in parts of the region for the foreseeable future (NOAA NCEI 2019). This warming trend—which is widely acknowledged as a global phenomenon (Cook and others 2016, Rahmstorf and others 2017)—has also contributed to the emergence of drought in the Pacific Northwest region, as decreased summer and fall precipitation as well as increased potential evapotranspiration have resulted in larger moisture deficits than the region experienced historically (Abatzoglou and others 2014).

Decreases in drought extent and severity in the southern portion of California in 2018 (fig. 4.2) relative to 2017 (fig. 4.3), particularly in sections M262B–Southern California Mountain and Valley and M261E–Sierra Nevada, may seem noteworthy for a region that recently has experienced dramatic forest health impacts due to drought. Between 2010 and 2017, more than 129 million trees in California were killed by direct or indirect drought effects (Buluç and others 2017). In the central and southern Sierra Nevada Mountains, tree mortality approached 50 percent overall and 90 percent for ponderosa pine (*Pinus ponderosa*) (Fettig and others 2019). Nevertheless, the apparent improvement in moisture conditions in California during 2018

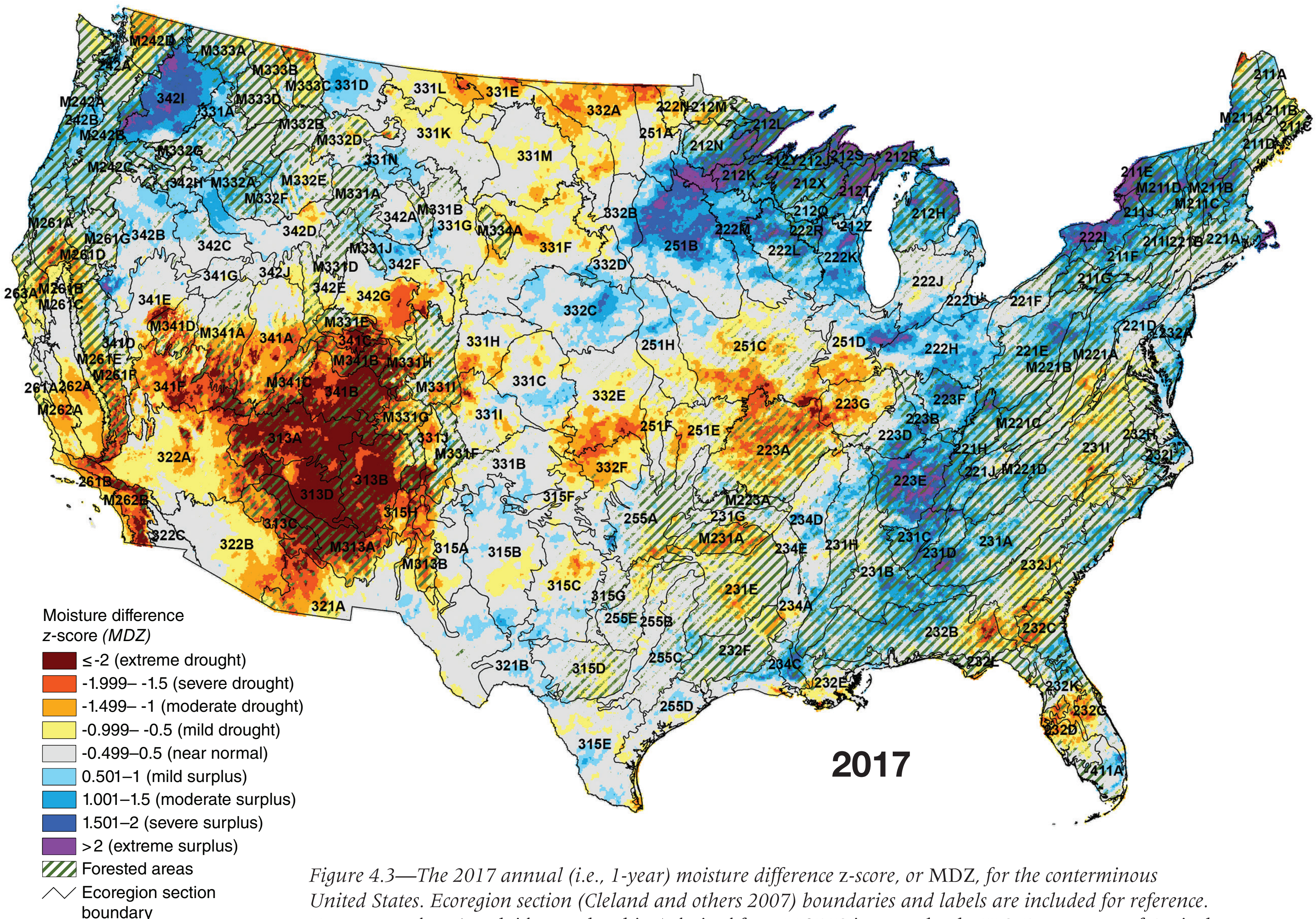

Figure 4.3—The 2017 annual (i.e., 1-year) moisture difference z-score, or MDZ, *for the conterminous United States. Ecoregion section (Cleland and others 2007) boundaries and labels are included for reference. Forest cover data (overlaid green hatching) derived from MODIS imagery by the U.S. Department of Agriculture Forest Service, Remote Sensing Applications Center. (Data source: PRISM Group, Oregon State University)*

must be viewed in the context of predictions that the State's moisture regime will be increasingly volatile in the future, with both extreme droughts and extreme wet events expected to become more frequent (Swain and others 2018). As is the case elsewhere, this volatility is likely to develop as a consequence of warming temperatures (Ullrich and others 2018). However, California's Mediterranean climate (i.e., dry summers and wet winters) makes it especially susceptible to abrupt swings between moisture extremes (Swain and others 2018).

Even in the face of warming temperatures, areas of persistent and intense drought have remained uncommon in the Eastern United States. For example, nearly all areas in the East that experienced moderate or worse drought conditions during 2017 (fig. 4.3) saw a return to near normal or even moisture surplus conditions in 2018 (fig. 4.2), although the aforementioned area of drought in northern New England became more extensive. The 3-year (2016–2018; fig. 4.4) and 5-year (2014–2018; fig. 4.5) *MDZ* maps serve as further illustration of the relative infrequency of prolonged droughts (i.e., spanning multiple years) in the East. The only notable areas of the Eastern United States where moderate or worse drought conditions (*MDZ* ≤-1) occurred in both the 3- and 5-year *MDZ* maps were in section 411A–Everglades, in very small portions of 232C–Atlantic Coastal Flatwoods and 232G–Florida Coastal Lowlands-Atlantic, and along the coastline of Maine (sections 211C–Fundy Coastal and Interior and 211D–Central Maine Coastal and Embayment). In the 3-year *MDZ* map (fig. 4.4), clusters of moderate or worse drought conditions also occurred in sections 223A–Ozark Highlands, 251C–Central Dissected Till Plains, 315F–Northern Texas High Plains, and 322F–South Central and Red Bed Plains. These clusters were much less prominent in the 5-year map (fig. 4.5), indicating that the drought conditions developed primarily within the last few years and probably were preceded by near-normal conditions in 2014–2015. Furthermore, only one of these sections (i.e., 223A) contains much forest.

In contrast, nearly all forested areas in the Western United States have experienced moderate or worse drought conditions that have persisted over multiple consecutive years. Outside of the Four Corners region, most of these areas exhibited lower *MDZ* values in the 5-year map than in the 3-year map, suggesting that moisture conditions improved in the 2016–2018 period relative to 2014–2015. Still, the near-ubiquity of drought conditions in Western U.S. forests—circumstances that extend back several decades in some parts of the West (Groisman and Knight 2008, Mueller and others 2005, Woodhouse and others 2010)—has undeniable implications for long-term forest health.

Areas of moisture surplus depicted in the 3-year (fig. 4.4) and 5-year (fig. 4.5) *MDZ* maps further underscore some dramatic differences between the Eastern and Western United States. Strikingly, the maps show almost no areas of severe to extreme moisture surplus

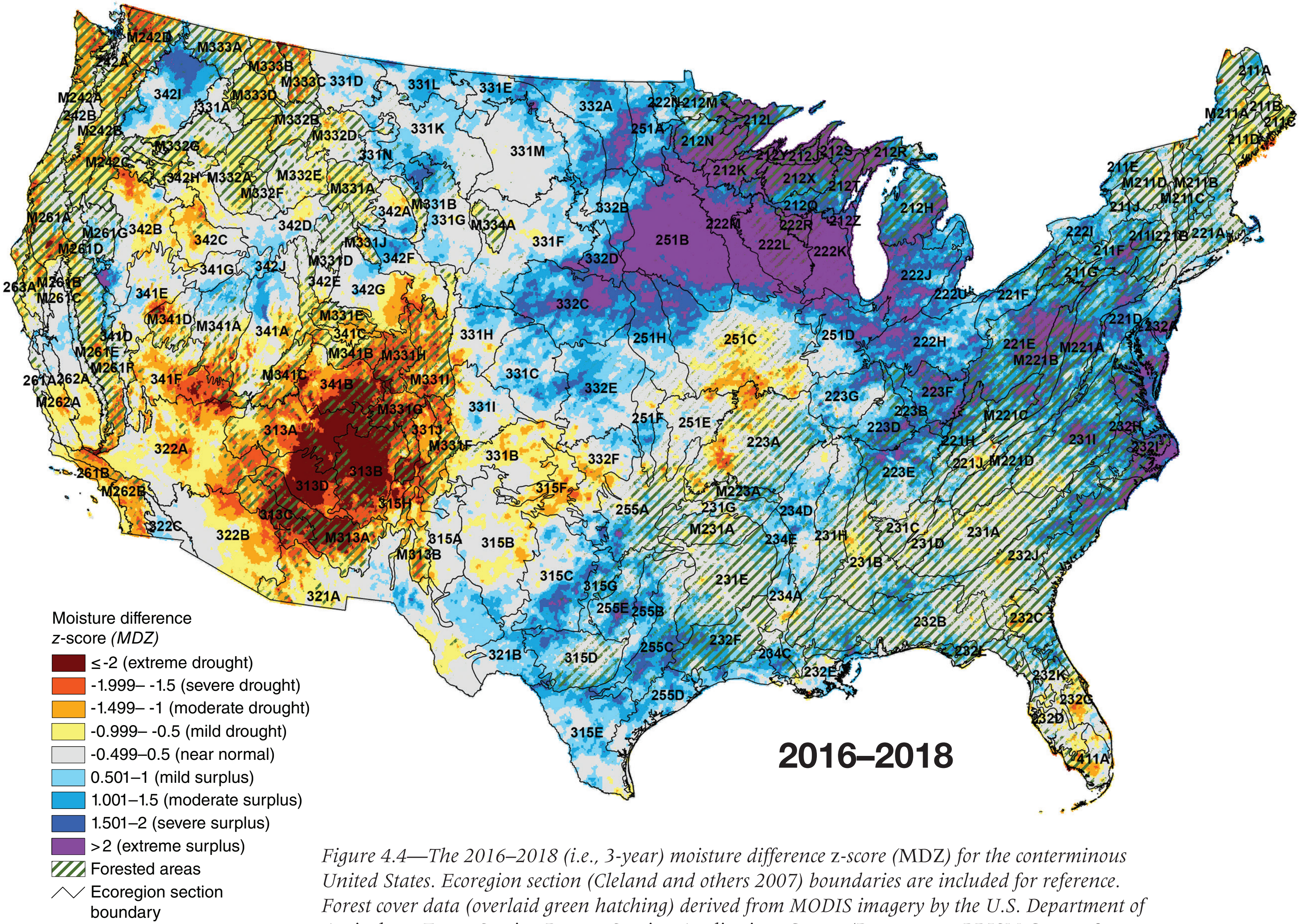

Figure 4.4—The 2016–2018 (i.e., 3-year) moisture difference z-score (MDZ) for the conterminous United States. Ecoregion section (Cleland and others 2007) boundaries are included for reference. Forest cover data (overlaid green hatching) derived from MODIS imagery by the U.S. Department of Agriculture Forest Service, Remote Sensing Applications Center. (Data source: PRISM Group, Oregon State University)

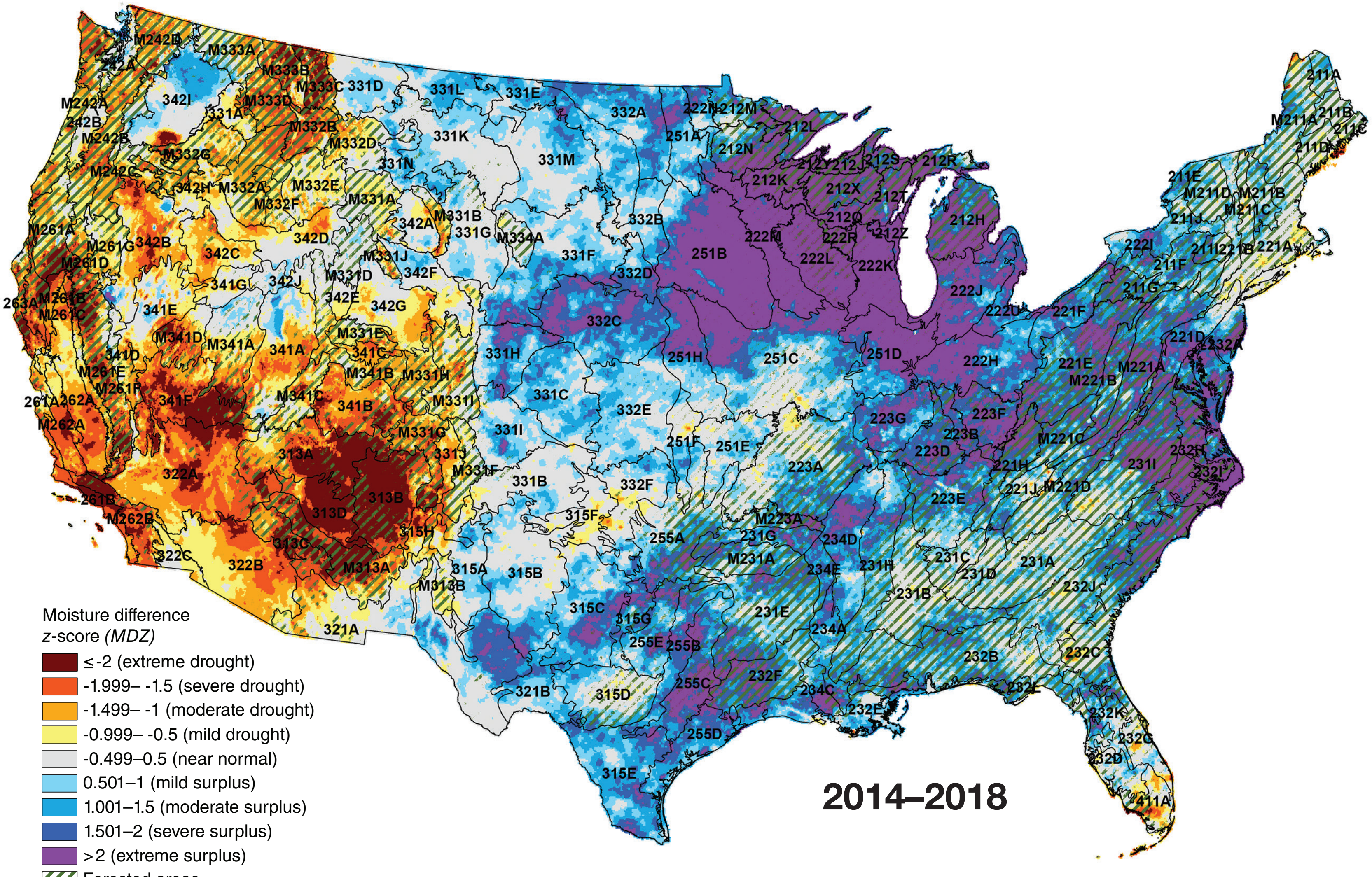

Figure 4.5—The 2014–2018 (i.e., 5-year) moisture difference z-score (MDZ) for the conterminous United States. Ecoregion section (Cleland and others 2007) boundaries are included for reference. Forest cover data (overlaid green hatching) derived from MODIS imagery by the U.S. Department of Agriculture Forest Service, Remote Sensing Applications Center. (Data source: PRISM Group, Oregon State University)

west of the Rocky Mountains. The solitary exception is in the southwestern corner of section 342B–Northwestern Basin and Range, an area that has little forest. In addition, the northern portion of 342I–Columbia Basin showed a severe moisture surplus in the 3-year *MDZ* map (fig. 4.4) but only moderate surplus in the 5-year map (fig. 4.5). By comparison, a nearly continuous swath of severe to extreme moisture surplus stretched across much of the Eastern United States in both the 3- and 5-year maps, from the western Great Lakes region (e.g., forested sections 212J–Southern Superior Uplands, 212K–Western Superior Uplands, 212Q–North Central Wisconsin Uplands, 212R–Eastern Upper Peninsula, 212X–Northern Highlands, 212Y–Southwest Lake Superior Clay Plain, 222L–North Central U.S. Driftless and Escarpment, and 222R–Wisconsin Central Sands) to eastern North Carolina and South Carolina (e.g., sections 231I–Central Appalachian Piedmont, 232C–Atlantic Coastal Flatwoods, 232H–Middle Atlantic Coastal Plains and Flatwoods, and 232I–Northern Atlantic Coastal Flatwoods). The geographic footprint of the swath was close to identical in the two maps. Another contiguous area of moisture surplus covered parts of Louisiana and Texas (e.g., sections 231E–Mid Coastal Plains-Western, 232F–Coastal Plains and Flatwoods-Western Gulf, 234C–Atchafalaya and Red River Alluvial Plains, 255A–Cross Timbers and Prairie, 255B–Blackland Prairies, 255C–Oak Woods and Prairies, 255E–Texas Cross Timbers and Prairie, and 315G–Eastern Rolling Plains). In general, the 3-year *MDZ* map showed a lower degree of moisture surplus in this area than the 5-year map, which may signal an ongoing shift from surplus to drought conditions.

The forest health impacts of these prolonged surpluses are unclear. Localized damage due to flooding is reasonably common in U.S. forests, but impacts related to surplus conditions more broadly are not well documented. Recent research has suggested that persistent excess moisture can increase vulnerability of forests to pathogens and other disease-causing agents (Hubbart and others 2016). These agents may be further enabled during times of high climate variability, such as when a period of drought occurs immediately before or after a period of moisture surplus, or when wet and warm conditions co-occur (Hubbart and others 2016). Despite the uncertainty, continued monitoring is advisable for the areas of persistent moisture surplus identified in the 3- and 5-year *MDZ* maps.

Future Efforts

We intend to provide 1-year, 3-year, and 5-year *MDZ* maps of the conterminous United States as an annually recurring component of national forest health reporting. To interpret the maps appropriately, it is critical to recognize their limitations. Foremost, the *MDZ* approach omits some factors that can affect a location's moisture supply at a finer spatial scale, such as winter snowpack, surface runoff, or groundwater storage. Moreover, while the maps use a standardized index scale that applies to time windows of any size, it is still important to choose a window size that is analytically appropriate. For example, an extreme drought that lasts for 5 years will have substantially different forest health ramifications than an extreme drought that ends after only 1 year. We believe the 1-year, 3-year, and 5-year *MDZ* maps provide a fairly comprehensive short-term picture, but a region's longer term moisture history may also be meaningful with respect to the health of its forests. For instance, in regions where droughts have been frequent historically (e.g., occurring on an annual or nearly annual basis), some tree species may be better drought-adapted than others (McDowell and others 2008); because of this variability, long periods of persistent and intense drought conditions could lead to eventual changes in regional forest composition (Mueller and others 2005). Compositional changes may also emerge from long periods of persistent moisture surplus (McEwan and others 2011). Such changes are likely to affect regional responses to future drought or surplus conditions, fire regimes, and the status of ecosystem services such as nutrient cycling and wildlife habitat (W.R.L. Anderegg and others 2013, DeSantis and others 2011). In future work, we hope to deliver better quantitative evidence to forest managers and other decisionmakers regarding relationships between moisture extremes and significant forest health impacts such as regional-scale tree mortality (e.g., Mitchell and others 2014). We also intend to investigate the capacity of moisture extremes to serve as inciting factors for other forest threats such as wildfire or pest outbreaks.

LITERATURE CITED

Abatzoglou, J.T.; Rupp, D.E.; Mote, P.W. 2014. Seasonal climate variability and change in the Pacific Northwest of the United States. Journal of Climate. 27(5): 2125–2142.

Adams, H.D.; Guardiola-Claramonte, M.; Barron-Gafford, G.A. [and others]. 2009. Temperature sensitivity of drought-induced tree mortality portends increased regional die-off under global-change-type drought. Proceedings of the National Academy of Sciences. 106(17): 7063–7066.

Akin, W.E. 1991. Global patterns: climate, vegetation, and soils. Norman, OK: University of Oklahoma Press. 370 p.

Allen, C.D.; Macalady, A.K.; Chenchouni, H. [and others]. 2010. A global overview of drought and heat-induced tree mortality reveals emerging climate change risks for forests. Forest Ecology and Management. 259(4): 660–684.

Alley, W.M. 1984. The Palmer Drought Severity Index: limitations and assumptions. Journal of Climate and Applied Meteorology. 23: 1100–1109.

Anderegg, L.D.L.; Anderegg, W.R.L.; Berry, J.A. 2013. Not all droughts are created equal: translating meteorological drought into woody plant mortality. Tree Physiology. 33(7): 672–683.

Anderegg, W.R.L.; Berry, J.A.; Field, C.B. 2012. Linking definitions, mechanisms, and modeling of drought-induced tree death. Trends in Plant Science. 17(12): 693–700.

Anderegg, W.R.L.; Kane, J.M.; Anderegg, L.D.L. 2013. Consequences of widespread tree mortality triggered by drought and temperature stress. Nature Climate Change. 3(1): 30–36.

Archaux, F.; Wolters, V. 2006. Impact of summer drought on forest biodiversity: what do we know? Annals of Forest Science. 63: 645–652.

Berdanier, A.B.; Clark, J.S. 2016. Multiyear drought-induced morbidity preceding tree death in southeastern U.S. forests. Ecological Applications. 26(1): 17–23.

Bigler, C.; Bräker, O.U.; Bugmann, H. [and others]. 2006. Drought as an inciting mortality factor in Scots pine stands of the Valais, Switzerland. Ecosystems. 9(3): 330–343.

Buluç, L.; Fischer, C.; Ko, J. [and others]. 2017. Drought and tree mortality in the Pacific Southwest region. [Fact sheet]. Washington, D.C.: U.S. Department of Agriculture Forest Service, Office of Sustainability and Climate. 14 p.

Choat, B.; Brodribb, T.J.; Brodersen, C.R. [and others]. 2018. Triggers of tree mortality under drought. Nature. 558(7711): 531–539.

Clark, J.S. 1989. Effects of long-term water balances on fire regime, north-western Minnesota. Journal of Ecology. 77: 989–1004.

Cleland, D.T.; Freeouf, J.A.; Keys, J.E. [and others]. 2007. Ecological subregions: sections and subsections for the conterminous United States. Gen. Tech. Rep. WO-76D. Washington, DC: U.S. Department of Agriculture Forest Service. Map; Sloan, A.M., cartographer; presentation scale 1:3,500,000; colored. Also on CD-ROM as a GIS coverage in ArcINFO format.

Clinton, B.D.; Boring, L.R.; Swank, W.T. 1993. Canopy gap characteristics and drought influences in oak forests of the Coweeta Basin. Ecology. 74(5): 1551–1558.

Cook, J.; Oreskes, N.; Doran, P.T. [and others]. 2016. Consensus on consensus: a synthesis of consensus estimates on human-caused global warming. Environmental Research Letters. 11(4): 048002.

Daly, C.; Gibson, W.P.; Taylor, G.H. [and others]. 2002. A knowledge-based approach to the statistical mapping of climate. Climate Research. 22: 99–113.

DeSantis, R.D.; Hallgren, S.W.; Stahle, D.W. 2011. Drought and fire suppression lead to rapid forest composition change in a forest-prairie ecotone. Forest Ecology and Management. 261(11): 1833–1840.

Duever, M.J.; Meeder, J.F.; Meeder, L.C.; McCollum, J.M. 1994. The climate of south Florida and its role in shaping the Everglades ecosystem. In: Davis, S.M.; Ogden, J.C., eds. Everglades: the ecosystem and its restoration. Delray Beach, FL: St. Lucie Press: 225–248.

Fettig, C.J.; Mortenson, L.A.; Bulaon, B.M.; Foulk, P.B. 2019. Tree mortality following drought in the central and southern Sierra Nevada, California, U.S. Forest Ecology and Management. 432: 164–178.

Groisman, P.Y.; Knight, R.W. 2008. Prolonged dry episodes over the conterminous United States: new tendencies emerging during the last 40 years. Journal of Climate. 21: 1850–1862.

Grundstein, A. 2009. Evaluation of climate change over the continental United States using a moisture index. Climatic Change. 93: 103–115.

Guarín, A.; Taylor, A.H. 2005. Drought triggered tree mortality in mixed conifer forests in Yosemite National Park, California, USA. Forest Ecology and Management. 218: 229–244.

Hanson, P.J.; Weltzin, J.F. 2000. Drought disturbance from climate change: response of United States forests. The Science of the Total Environment. 262: 205–220.

Hubbart, J.A.; Guyette, R.; Muzika, R.M. 2016. More than drought: precipitation variance, excessive wetness, pathogens and the future of the western edge of the Eastern Deciduous Forest. Science of The Total Environment. 566–567: 463–467.

Kareiva, P.M.; Kingsolver, J.G.; Huey, B.B., eds. 1993. Biotic interactions and global change. Sunderland, MA: Sinauer Associates, Inc. 559 p.

Keetch, J.J.; Byram, G.M. 1968. A drought index for forest fire control. Res. Pap. SE-38. Asheville, NC: U.S. Department of Agriculture Forest Service, Southeastern Forest Experiment Station. 33 p.

Koch, F.H.; Coulston, J.W. 2015. 1-year (2013), 3-year (2011–2013), and 5-year (2009–2013) drought maps for the conterminous United States. In: Potter, K.M.; Conkling, B.L., eds. Forest Health Monitoring: national status, trends, and analysis 2014. Gen. Tech. Rep. SRS-209. Asheville, NC: U.S. Department of Agriculture Forest Service, Southern Research Station: 57–71. Chapter 4.

Koch, F.H.; Coulston, J.W. 2016. 1-year (2014), 3-year (2012–2014), and 5-year (2010–2014) maps of drought and moisture surplus for the conterminous United States. In: Potter, K.M.; Conkling, B.L., eds. Forest Health Monitoring: national status, trends, and analysis 2015. Gen. Tech. Rep. SRS-213. Asheville, NC: U.S. Department of Agriculture Forest Service, Southern Research Station: 61–78. Chapter 4.

Koch, F.H.; Coulston, J.W. 2017. Moisture deficit and surplus in the conterminous United States for three time windows: 2015, 2013–2015, and 2011–2015. In: Potter, K.M.; Conkling, B.L., eds. Forest Health Monitoring: national status, trends, and analysis 2016. Gen. Tech. Rep. SRS-222. Asheville, NC: U.S. Department of Agriculture Forest Service, Southern Research Station: 63–80. Chapter 4.

Koch, F.H.; Coulston, J.W. 2018. Moisture deficit and surplus in the conterminous United States for three time windows: 2016, 2014–2016, and 2012–2016. In: Potter, K.M.; Conkling, B.L., eds. Forest Health Monitoring: national status, trends, and analysis 2017. Gen. Tech Rep. SRS-233. Asheville, NC: U.S. Department of Agriculture Forest Service, Southern Research Station: 65–84. Chapter 4.

Koch, F.H.; Coulston, J.W. 2019. Drought and moisture surplus patterns in the conterminous United States: 2017, 2015–2017, and 2013–2017. In: Potter, K.M.; Conkling, B.L., eds. Forest Health Monitoring: national status, trends, and analysis 2018. Gen. Tech Rep. SRS-239. Asheville, NC: U.S. Department of Agriculture Forest Service, Southern Research Station: 77–96. Chapter 4.

Koch, F.H.; Coulston, J.W.; Smith, W.D. 2012a. High-resolution mapping of drought conditions. In: Potter, K.M.; Conkling, B.L., eds. Forest Health Monitoring 2008 national technical report. Gen. Tech. Rep. SRS-158. Asheville, NC: U.S. Department of Agriculture Forest Service, Southern Research Station: 45–62. Chapter 4.

Koch, F.H.; Coulston, J.W.; Smith, W.D. 2012b. Mapping drought conditions using multi-year windows. In: Potter, K.M.; Conkling, B.L., eds. Forest Health Monitoring 2009 national technical report. Gen. Tech. Rep. SRS-167. Asheville, NC: U.S. Department of Agriculture Forest Service, Southern Research Station: 163–179. Chapter 10.

Koch, F.H.; Smith, W.D.; Coulston, J.W. 2013a. Recent drought conditions in the conterminous United States. In: Potter, K.M.; Conkling, B.L., eds. Forest Health Monitoring: national status, trends, and analysis 2011. Gen. Tech. Rep. SRS-185. Asheville, NC: U.S. Department of Agriculture Forest Service, Southern Research Station: 41–58. Chapter 4.

Koch, F.H.; Smith, W.D.; Coulston, J.W. 2013b. An improved method for standardized mapping of drought conditions. In: Potter, K.M.; Conkling, B.L., eds. Forest Health Monitoring: national status, trends, and analysis 2010. Gen. Tech. Rep. SRS-176. Asheville, NC: U.S. Department of Agriculture Forest Service, Southern Research Station: 67–83. Chapter 6.

Koch, F.H.; Smith, W.D.; Coulston, J.W. 2014. Drought patterns in the conterminous United States and Hawaii. In: Potter, K.M.; Conkling, B.L., eds. Forest Health Monitoring: national status, trends, and analysis 2012. Gen. Tech. Rep. SRS-198. Asheville, NC: U.S. Department of Agriculture Forest Service, Southern Research Station: 49–72. Chapter 4.

Koch, F.H.; Smith, W.D.; Coulston, J.W. 2015. Drought patterns in the conterminous United States, 2012. In: Potter, K.M.; Conkling, B.L., eds. Forest Health Monitoring: national status, trends, and analysis 2013. Gen. Tech. Rep. SRS-207. Asheville, NC: U.S. Department of Agriculture Forest Service, Southern Research Station: 55–69. Chapter 4.

Kolb, T.E.; Fettig, C.J.; Ayres, M.P. [and others]. 2016. Observed and anticipated impacts of drought on forest insects and diseases in the United States. Forest Ecology and Management. 380: 321–334.

Laurance, S.G.W.; Laurance, W.F.; Nascimento, H.E.M. [and others]. 2009. Long-term variation in Amazon forest dynamics. Journal of Vegetation Science. 20(2): 323–333.

Martínez-Vilalta, J.; Lloret, F.; Breshears, D.D. 2012. Drought-induced forest decline: causes, scope and implications. Biology Letters. 8(5): 689–691.

Mattson, W.J.; Haack, R.A. 1987. The role of drought in outbreaks of plant-eating insects. BioScience. 37(2): 110–118.

McDowell, N.; Pockman, W.T.; Allen, C.D. [and others]. 2008. Mechanisms of plant survival and mortality during drought: why do some plants survive while others succumb to drought? New Phytologist. 178: 719–739.

McEwan, R.W.; Dyer, J.M.; Pederson, N. 2011. Multiple interacting ecosystem drivers: toward an encompassing hypothesis of oak forest dynamics across eastern North America. Ecography. 34: 244–256.

McKee, T.B.; Doesken, N.J.; Kleist, J. 1993. The relationship of drought frequency and duration to time scales. In: Eighth conference on applied climatology. [Place of publication unknown]: American Meteorological Society: 179–184.

Millar, C.I.; Westfall, R.D.; Delany, D.L. 2007. Response of high-elevation limber pine (*Pinus flexilis*) to multiyear droughts and 20th-century warming, Sierra Nevada, California, USA. Canadian Journal of Forest Research. 37: 2508–2520.

Mitchell, P.J.; O'Grady, A.P.; Hayes, K.R.; Pinkard, E.A. 2014. Exposure of trees to drought-induced die-off is defined by a common climatic threshold across different vegetation types. Ecology and Evolution. 4(7): 1088–1101.

Monteith, J.L. 1965. Evaporation and environment. Symposia of the Society for Experimental Biology. 19: 205–234.

Mueller, R.C.; Scudder, C.M.; Porter, M.E. [and others]. 2005. Differential tree mortality in response to severe drought: evidence for long-term vegetation shifts. Journal of Ecology. 93: 1085–1093.

National Oceanic and Atmospheric Administration (NOAA) National Centers for Environmental Information (NCEI). 2019. State of the climate: drought for annual 2018. https://www.ncdc.noaa.gov/sotc/drought/201813. [Date accessed: August 22, 2019].

Palmer, W.C. 1965. Metereological drought. Washington, DC: U.S. Department of Commerce Weather Bureau. 58 p.

Peng, C.; Ma, Z.; Lei, X. [and others]. 2011. A drought-induced pervasive increase in tree mortality across Canada's boreal forests. Nature Climate Change. 1(9): 467–471.

Peters, M.P.; Iverson, L.R.; Matthews, S.N. 2015. Long-term droughtiness and drought tolerance of eastern US forests over five decades. Forest Ecology and Management. 345: 56–64.

Potter, C.S.; Klooster, S.A. 1999. Dynamic global vegetation modelling for prediction of plant functional types and biogenic trace gas fluxes. Global Ecology and Biogeography. 8(6): 473–488.

PRISM Climate Group. 2019. 2.5-arcmin (4 km) gridded monthly climate data. http://www.prism.oregonstate.edu. [Date accessed: August 1, 2019].

Raffa, K.F.; Aukema, B.H.; Bentz, B.J. [and others]. 2008. Cross-scale drivers of natural disturbances prone to anthropogenic amplification: the dynamics of bark beetle eruptions. BioScience. 58(6): 501–517.

Rahmstorf, S.; Foster, G.; Cahill, N. 2017. Global temperature evolution: recent trends and some pitfalls. Environmental Research Letters. 12(5): 054001.

Rozas, V.; García-González, I. 2012. Too wet for oaks? Inter-tree competition and recent persistent wetness predispose oaks to rainfall-induced dieback in Atlantic rainy forest. Global and Planetary Change. 94–95: 62–71.

Rozas, V.; Sampedro, L. 2013. Soil chemical properties and dieback of *Quercus robur* in Atlantic wet forests after a weather extreme. Plant and Soil. 373(1–2): 673–685.

Schoennagel, T.; Veblen, T.T.; Romme, W.H. 2004. The interaction of fire, fuels, and climate across Rocky Mountain forests. BioScience. 54(7): 661–676.

Slette, I.J.; Post, A.K.; Awad, M. [and others]. 2019. How ecologists define drought, and why we should do better. Global Change Biology. 25(10): 3193–3200.

Steinemann, A. 2003. Drought indicators and triggers: a stochastic approach to evaluation. Journal of the American Water Resources Association. 39(5): 1217–1233.

Svoboda, M.; LeComte, D.; Hayes, M. [and others]. 2002. The drought monitor. Bulletin of the American Meteorological Society. 83(8): 1181–1190.

Swain, D.L.; Langenbrunner, B.; Neelin, J.D.; Hall, A. 2018. Increasing precipitation volatility in twenty-first-century California. Nature Climate Change. 8(5): 427–433.

Thornthwaite, C.W. 1948. An approach towards a rational classification of climate. Geographical Review. 38(1): 55–94.

Thornthwaite, C.W.; Mather, J.R. 1955. The water balance. Publications in Climatology. 8(1): 1–104.

Trouet, V.; Taylor, A.H.; Wahl, E.R. [and others]. 2010. Fire-climate interactions in the American West since 1400 CE. Geophysical Research Letters. 37(4): L04702.

Ullrich, P.A.; Xu, Z.; Rhoades, A.M. [and others]. 2018. California's drought of the future: a midcentury recreation of the exceptional conditions of 2012–2017. Earth's Future. 6(11): 1568–1587.

Vose, R.S.; Applequist, S.; Squires, M. [and others]. 2014. Improved historical temperature and precipitation time series for U.S. climate divisions. Journal of Applied Meteorology and Climatology. 53(5): 1232–1251.

Williams, A.P.; Allen, C.D.; Macalady, A.K. [and others]. 2013. Temperature as a potent driver of regional forest drought stress and tree mortality. Nature Climate Change. 3(3): 292–297.

Willmott, C.J.; Feddema, J.J. 1992. A more rational climatic moisture index. Professional Geographer. 44(1): 84–87.

Woodhouse, C.A.; Meko, D.M.; MacDonald, G.M. [and others]. 2010. A 1,200-year perspective of 21st century drought in southwestern North America. Proceedings of the National Academy of Sciences. 107(50): 21283–21288.